V International Scientific and Technical Conference Actual Issues of Power Supply Systems

Load Operating Modes of a Ferromagnetic Current Stabilizer in Magnetic Amplifier Control Circuits

AIPCP25-CF-ICAIPSS2025-00622 | Article

Load Operating Modes of a Ferromagnetic Current Stabilizer in Magnetic Amplifier Control Circuits

Ikromjon Rakhmonov[1,3], Abdulhay Rasulov[1], Mirjalol Ruzinazarov[1, a)],
Ullibibi Sabirova [2], Abdubakir Abdullaev [2]

[1] *Tashkent state technical university named after Islam Karimov, Tashkent, Uzbekistan*
[2] *Tashkent university of information technologies named after Muhammad al-Khwarizmi, Tashkent, Uzbekistan*
[3] *Termiz State University of Engineering and Agrotechnology, Termez, Uzbekistan*

[a)] *Corresponding author: ruzinzarov88@bk.ru*

Abstract. This paper presents a comprehensive analysis of the load operating modes of a ferromagnetic current stabilizer used in the control circuits of magnetic amplifiers. Stable operating regimes for resistive, resistive–inductive, and resistive–capacitive loads are investigated using mathematical modeling and graphical–analytical methods. The results show that a resistive–capacitive load is the most favorable option for current stabilization, providing a wider stabilization range. In addition, the harmonic content of the stabilized current is analyzed, revealing a significant degree of nonlinearity in the current waveform. The obtained results confirm the feasibility and effectiveness of using ferromagnetic current stabilizers in low-power control and stabilization systems.

INTRODUCTION

In industrial and power engineering systems, electromagnetic devices based on magnetic amplifiers play a significant role in automatic control and stabilization applications. In particular, the energy efficiency and reliability of current stabilization circuits used in the control circuits of such devices are of great relevance in view of modern technical requirements [1-5]. Although current stabilizers based on ferroresonant circuits exhibit high stabilization capability, their application in high-power systems is limited due to the fact that the installed capacity of reactive elements exceeds the load power by several times. Therefore, the use of such circuits is considered most appropriate in the control circuits of magnetic amplifiers where only low power levels are required [6-10]. When a ferromagnetic current stabilizer (FCS) is employed in the control circuit of a magnetic amplifier, it represents a unique electromagnetic device that combines the advantages of a ferroresonant circuit and a magnetic amplifier.

EXPERIMENTAL RESEARCH

Such a dependence qualitatively describes the characteristic of simultaneous magnetization in the operating region of the magnetic amplifier under stabilization conditions and provides sufficiently simple results for analyzing the load operating regime of the device (Figure 1). The value of the coefficient depends on the magnitude of the bias current and can be determined using the method of selected points or the least squares method.

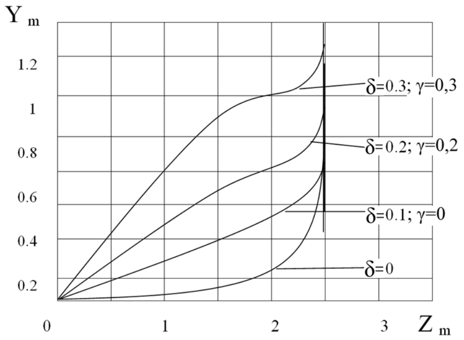

FIGURE 1. Regulation characteristics for a resistive – capacitive load

$$\gamma = \frac{i_\delta}{2\omega^3 W C_H \phi_\delta} \tag{1}$$

Thus, expressions (1) and (2) differ from each other only in the signs preceding the coefficients γ_H and γ, which are proportional to the inductive and capacitive impedances of the loads, respectively. Figure 2 illustrates the nature of variation of the regulation characteristics for different values of complex loads [11-14]. From this, it can be concluded that a resistive–capacitive load is more favorable for the current stabilization mode, since the voltage stabilization range is wider compared to the inductive type of load when identical values of δ and γ are assumed.

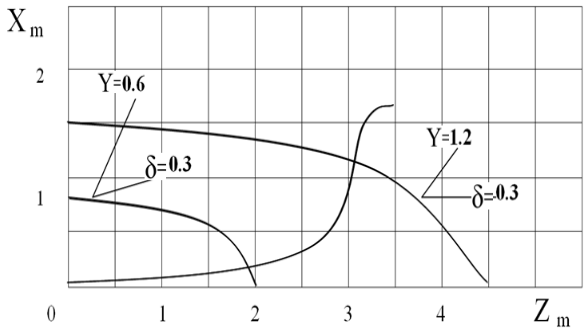

FIGURE 2. Dependence $X_m=f(Z_m)$.

Let us consider the application of the graphical–analytical method to the analysis of a ferromagnetic current stabilizer circuit for the case of a complex load. We assume that the characteristic $X_m=f(Z_m)$ of the current stabilizer circuit is known [15-17]. This characteristic can be determined on the basis of the magnetization curve of the ferromagnetic element and the characteristic of the compensating capacitance.

$$u = L_H \frac{at_{ct}}{dt} + r_H i_{ct} + 2W \frac{a\phi}{dt} \tag{2}$$

After introducing normalized variables and taking into account equation (3), we obtain:

$$Y_m^2 = (\delta^2 + \gamma_H) Z_{mct}^2 + X_m^2 + 2\gamma_H Z_{mct} X_m \tag{3}$$

If $\gamma_H = 0$

$$Y_m^2 = \delta^2 Z_{mct}^2 + X_m^2 \tag{4}$$

and

$$\frac{z_{mct}^2}{\frac{z_{mct}^2}{\delta^2}} + \frac{x_m^2}{y_m^2} = 1 \tag{5}$$

RESEARCH RESULTS

From this it follows that, for a resistive load, the current of the ferromagnetic current stabilizer and the magnetic flux are related by an equation of an ellipse whose axes coincide with the axes of the coordinate system. On the other hand, these quantities are also related through the characteristic of the ferromagnetic current stabilizer circuit. Thus, by superimposing the ellipse onto the circuit characteristic of the ferroresonant current stabilizer, the operating regime can be determined [19-22]. The abscissa of the intersection point of the ellipse with the circuit characteristic indicates the value of the operating current, while the ordinate corresponds to the magnetic flux in the core of the ferromagnetic element (Fig. 3). If $\gamma \neq 0$, Z_m, X_m the quantities are also related by an ellipse equation whose center coincides with the origin of the coordinate system [18-22]. In this case, the ellipse axis is inclined at a certain angle with respect to the coordinate axes (Figure 4). Using the previously discussed methodology, equation (14) can be written in the following form.

$$\frac{z_m^2}{\frac{y_m^2}{A}} + \frac{x_m^2}{\frac{y_m^2}{C}} = 1 \tag{6}$$

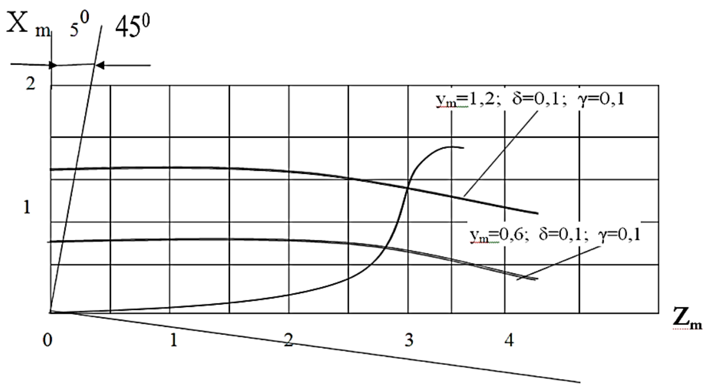

FIGURE 3. Dependence $X_m=f(Z_{.m})$ $\gamma \neq 0$

Here

$$A = (\delta^2 + \gamma_H^2)\cos^2\alpha + \sin^2\alpha + 2\gamma_H \sin\alpha\cos\alpha \tag{7}$$

$$C = (\delta^2 + \gamma_H^2)\sin^2\alpha + \cos^2\alpha + 2\gamma_H \sin\alpha\cos\alpha \tag{8}$$

$$tg\alpha = \frac{2\gamma}{\delta^2 + \gamma_H - 1} \tag{9}$$

Here, α is the angle of rotation of the ellipse axes, and Z_m, X_m are the new coordinates.

Figure 5 presents ellipses corresponding to different values of the input voltage for an inductive load, along with the dependence $Z_m=f(X_m)$ of the ferromagnetic current stabilizer circuit. In this case, the angle α has a negative sign, which indicates a clockwise rotation of the coordinate system of the ellipse axes.

When the load has a resistive–capacitive character, the state equation of the circuit takes the following form:

$$\frac{du}{dt} = \frac{i}{c} + R\frac{di}{dt} + 2W\frac{d^2\phi}{dt^2} \tag{10}$$

$$Y_m^2 = (\delta^2 + \gamma^2)X_m^2 + X_m^2 + 2\gamma X_m X_m \tag{11}$$

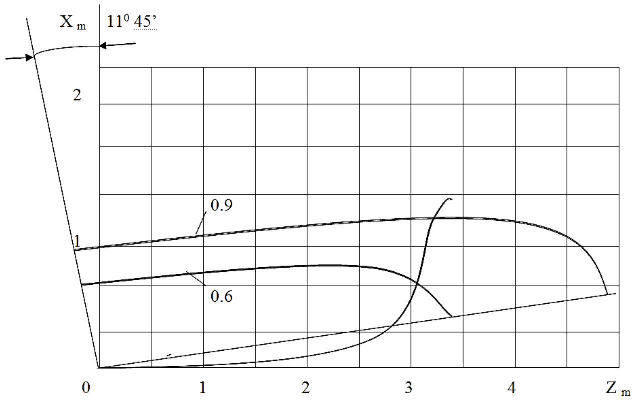

FIGURE 4. Dependence $X_m=f(Z_m)$ for the case $\gamma \neq 0$

Further investigation of dependence () has shown that expressions analogous to (6), (7), (8), and (9) are also obtained in this case, differing only in the signs preceding the coefficients $\gamma_n$and γ. The angle of rotation of the ellipse axes has a positive sign. The advantage of analysis using the graphical–analytical method lies in the possibility of employing experimentally obtained characteristics of the device.

Harmonic content of the stabilized current. The curve of simultaneous magnetization of the ferromagnetic element is a strongly nonlinear characteristic; therefore, the waveform of the stabilized current differs from a sinusoidal shape. To evaluate the harmonic content, dependence (4.3) is used, which was derived for the case where the magnetic amplifier is connected to a sinusoidal voltage source.

$$z = \left(7x_0^6X_m + \frac{3*35}{4}x_0^4X_m^3 + \frac{21*10}{16}x_0^2X_m^5 + \frac{35}{64}X_m^7\right)sin\tau - \left(\frac{35}{4}x_0^4X_m^3 + \frac{21*5}{16}x_0^2X_m^5 + \frac{21}{64}X_m^7\right)sin3\tau + \left(\frac{21}{16}x_0^2X_m^5 + \frac{7}{64}X_m^7\right)sin5\tau - \frac{1}{64}X_m^7 sin7\tau \tag{12}$$

The stabilization current of the considered circuit is the sum of the currents of the magnetic amplifier and the capacitance Cк (Fig. 4). Therefore

$$Z_{ct} = \left(7x_0^6X_m + \frac{3*35}{4}x_0^4X_m^3 + \frac{21*10}{16}x_0^2X_m^5 + \frac{35}{64}X_m^7 - \frac{1}{m}X_m\right)sin\tau - \left(\frac{35}{4}x_0^4X_m^3 + + \frac{21*5}{16}x_0^2X_m^5 + \frac{21}{64}X_m^7\right)sin3\tau + \left(\frac{21}{16}x_0^2X_m^5 + \frac{7}{64}X_m^7\right)sin5\tau - \frac{1}{64}X_m^7 sin7\tau \tag{13}$$

Based on the latter expression, we calculate the total harmonic distortion (THD) coefficient of the stabilized bias current. The coefficient of nonlinear distortion is determined by the following formula:

$$K_{ni}^2 = \frac{Z_{3m}^2 + Z_{5m}^2 + Z_{7m}^2}{\left(Z_{1m} - \frac{X_m}{m}\right)^2 + Z_{3m}^2 + Z_{5m}^2 + Z_{7m}^2}, \tag{14}$$

where

$$Z_{1m} = 7x_0^6X_m + \frac{3\cdot 35}{4}x_0^4X_m^3 + \frac{21\cdot 10}{16}x_0^2X_m^5 + \frac{35}{64}X_m^7 - \frac{1}{m}X_m \tag{15}$$

$$Z_{1m} = \frac{35}{4} x_0^4 X_m^3 + \frac{105}{16} x_0^2 X_m^5 + \frac{21}{64} X_m^7 \tag{16}$$

$$Z_{5m} = \frac{21}{16} x_0^2 X_m^3 + \frac{21}{64} X_m^7 \tag{17}$$

$$Z_{7m} = \frac{X_m^7}{64} \tag{18}$$

In Fig. 5 (curve 1), the variation of the nonlinear distortion coefficient as a function of X_m is shown for Z_0=1,8 It can be seen that this indicator is worse compared to the nonlinear distortion coefficient of a ferroresonant current stabilizer. Therefore, it is recommended to use a ferromagnetic current stabilizer in cases where no strict requirement is imposed on the current waveform.

As follows from expressions (15), (16), and (17), in order to determine Z_m, the value of X_0 must be known. For this purpose, the approximate real roots of the following equation are found:

$$X_m^7 = \frac{21}{2} x_0^5 X_{1m}^2 + \frac{35 \cdot 3}{8} x_0^3 X_{1m}^4 + \frac{7 \cdot 10}{32} x_0 X_{1m}^6 - Z_0 = 0 \tag{19}$$

First, the interval containing the desired root is determined. It is verified that the left-hand side of equation (19) takes values of opposite signs at the boundaries of this interval. Subsequently, by applying one of the methods for refining an approximate root to a specified accuracy, the actual value of X_0 is determined. Then, using expressions (14), (15), (16), (17), and (18), the value of the nonlinear distortion coefficient is calculated as a function of the supply voltage.

As can be seen from Fig. K_{ni} *the nonlinear distortion coefficient* varies from 0 to 62% when X_m deviates from 0.5 to 1.2 for Z_0=1,8.

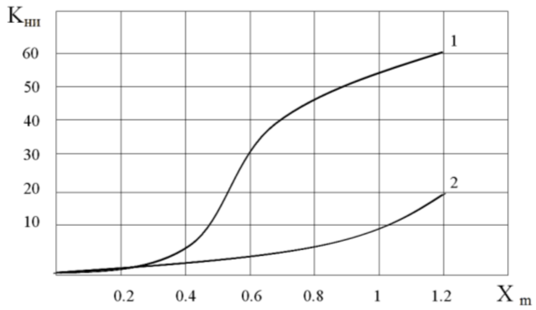

FIGURE 5. Dependence $K_{ni}=f(Z_m)$

CONCLUSION

The conducted research provides a detailed analysis of the operating modes of a ferromagnetic current stabilizer applied in the control circuits of magnetic amplifiers under various load conditions. The results of mathematical modeling demonstrate that the energy efficiency of the ferromagnetic current stabilizer is higher than that of conventional ferroresonant schemes, while the ratio of installed power to load power is significantly reduced. A comparative analysis of the regulation characteristics shows that a resistive–capacitive load is the most optimal for current stabilization, as it ensures a wider stabilization range. Overall, the developed mathematical model and analytical methods are effective tools for the design, optimization, and practical application of ferromagnetic current stabilizers and possess significant scientific and practical value for applied power engineering systems.

REFERENCES

1. T. Kadyrov. Electromagnetic ferro-circuits possessing a wide descending region on the amplitude–phase characteristic. *Proceedings of Higher Educational Institutions. Electromechanics*, 1988, No. 7, pp. 26–30.
2. D. Jumaeva, B. Numonov, N. Raxmatullaeva, M. Shamuratova. Obtaining of highly energy-efficient activated carbons based on wood, // E3S Web of Conferences 410, 01018, (2023). https://doi.org/10.1051/e3sconf/202341001018
3. M. Taniev, M. Hamdamov, A. Sotiboldiev, Power Losses Of Asynchronous Generators Based On Renewable Energy Sources E3S Web of Conferences, 434, 01020, (2023) https://doi.org/10.1051/e3sconf/202343401020
4. O. Toirov, S. Khalikov, Sodikjon Khalikov, F. Sharopov, Studies of reliability indicators of pumping units of machine irrigation on the example of the "Namangan" pumping station, // E3S Web of Conferences 410, 05015, (2023). https://doi.org/10.1051/e3sconf/202341005015
5. M. Rosenblat. *Magnetic Amplifiers with Self-Saturation*. Moscow: State Energy Publishing House (GEI), 1963, 127 p.
6. A. Rasulov, M. Melikuziev. Methodology for calculating electromagnetic ferro-circuits using approximation of the magnetization curve by a generalized n-th order function. *International Scientific Review*, No. 4 (II).
7. O. Toirov, T. Kamalov, U. Mirkhonov, S. Urokov, D. Jumaeva, The mathematical model and a block diagram of a synchronous motor compressor unit with a system of automatic control of the excitation // E3S Web of Conferences, 288, 01083, (2021), https://doi.org/10.1051/e3sconf/202128801083
8. D. Bystrov, S. Giyasov, M. Taniev, S. Urokov. Role of Reengineering in Training of Specialists // ACM International Conference Proceeding Series (2020) https://doi.org/10.1145/3386723.3387868
9. V. Ivanova, V. Tsypkina, D. Jumaeva, D. Abdullaeva, Improvement of the multifilament wire lager for cable production, // E3S Web of Conferences 411, 01041 (2023), https://doi.org/10.1051/e3sconf/202341101041
10. O. Toirov, S. Urokov, U. Mirkhonov, H. Afrisal, D. Jumaeva, Experimental study of the control of operating modes of a plate feeder based on a frequency-controlled electric drive, // E3S Web of Conferences, SUSE-2021, 288, 01086 (2021). https://doi.org/10.1051/e3sconf/202128801086
11. S. Khalikov, Diagnostics of pumping units of pumping station of machine water lifting, // E3S Web of Conferences 365, 04013, (2023). https://doi.org/10.1051/e3sconf/202336504013
12. M. Khalikova, D. Jumaeva, S. Kakharov, (2023) Development of a mathematical model of a frequency-controlled electromagnetic vibration motor taking into account the nonlinear dependences of the characteristics of the elements, // E3S Web of Conferences 401, 05089, (2023). https://doi.org/10.1051/e3sconf/202340105089
13. O. Toirov, S. Khalikov. Analysis of the safety of D. Bystrov, M. Gulzoda, Y. Dilfuza, Fuzzy Systems for Computational Linguistics and Natural Language (2020) // ACM International Conference Proceeding Series, https://doi.org/10.1145/3386723.3387873
14. I. Khujaev, J. Jumayev, M. Hamdamov, Modeling of vertical axis wind turbine using Ansys Fluent package program, // E3S Web of Conferences 401, 04040 (2023). https://doi.org/10.1051/e3sconf/202340104040
15. D. Jumaeva, A. Abdurakhimov, Kh. Abdurakhimov, N. Rakhmatullaeva, Energy of adsorption of an adsorbent in solving environmental problems, // E3S Web of Conferences, SUSE-2021, 288, 01082 (2021). https://doi.org/10.1051/e3sconf/202128801082
16. O. Toirov, D. Jumaeva, U. Mirkhonov, S. Urokov, S. Ergashev, Frequency-controlled asynchronous electric drives and their energy parameters, // AIP Conference Proceedings 2552, 040021, (2022). https://doi.org/10.1063/5.0218808
17. A. Rasulov, R. Ruzinazarov. Ferroresonant devices for current stabilization. *Universum: Technical Sciences*, No. 3–4, pp. 5–9, 2016.
18. V. Bedritsky. DC current stabilizers with a controlled inductive element in a ferroresonant circuit. In: *Proceedings of the XI International Scientific Conference "Current Issues of Modern Engineering and Technology"*, April 14, 2014, Lipetsk, Russia, pp. 77–81.
19. O. Toirov, T. Sadullaev, D. Abdullaev, D. Jumaeva, Sh. Ergashev, I.B. Sapaev, Development of contactless switching devices for asynchronous machines in order to save energy and resources, // E3S Web of Conferences 383, 01029, (2023). https://doi.org/10.1051/e3sconf/202338301029
20. S. Khalikov, Algorithm and Software Implementation of the Diagnostic System for the Technical Condition of Powerful Units, // E3S Web of Conferences 377, 01004, (2023). https://doi.org/10.1051/e3sconf/202337701004

21. D. Jumaeva, Z. Okhunjanov, U. Raximov, R. Akhrorova. Investigation of the adsorption of nonpolar adsorbate molecules on the illite surface, // Journal of Chemical Technology and Metallurgy, 58, 2, (2023). https://doi.org/10.59957/jctm.v58i2.61
22. O. Toirov, K. Alimkhodjaev, A. Pardaboev, Analysis and ways of reducing electricity losses in the electric power systems of industrial enterprises, // E3S Web of Conferences, SUSE-2021, 288, 01085 (2021). https://doi.org/10.1051/e3sconf/202128801085